COVID-19 Detection through Transfer Learning Using Multimodal Imaging Data

IEEE Access
Multidisciplinary | Rapid Review | Open Access Journal

Received August 6, 2020, accepted August 11, 2020, date of publication August 14, 2020, date of current version August 25, 2020.

Digital Object Identifier 10.1109/ACCESS.2020.3016780

COVID-19 Detection Through Transfer Learning Using Multimodal Imaging Data

MICHAEL J. HORRY[1,5], (Graduate Student Member, IEEE), SUBRATA CHAKRABORTY[1], (Senior Member, IEEE), MANORANJAN PAUL[2], (Senior Member, IEEE), ANWAAR ULHAQ[2], (Member, IEEE), BISWAJEET PRADHAN[1,4], (Senior Member, IEEE), MANAS SAHA[3], AND NAGESH SHUKLA[1]

[1]Centre for Advanced Modelling and Geospatial Information Systems (CAMGIS), School of Information, Systems, and Modeling, Faculty of Engineering and IT, University of Technology Sydney, Sydney, NSW 2007, Australia
[2]Machine Vision and Digital Health (MaViDH), School of Computing and Mathematics, Charles Sturt University, Bathurst, NSW 2795, Australia
[3]Manning Rural Referral Hospital, Taree, NSW 2430, Australia
[4]Department of Energy and Mineral Resources Engineering, Sejong University, Seoul 05006, South Korea
[5]IBM Australia Limited, Sydney, NSW 2065, Australia

Corresponding author: Subrata Chakraborty (subrata.chakraborty@uts.edu.au)

ABSTRACT Detecting COVID-19 early may help in devising an appropriate treatment plan and disease containment decisions. In this study, we demonstrate how transfer learning from deep learning models can be used to perform COVID-19 detection using images from three most commonly used medical imaging modes X-Ray, Ultrasound, and CT scan. The aim is to provide over-stressed medical professionals a second pair of eyes through intelligent deep learning image classi cation models. We identify a suitable *Convolutional Neural Network* (CNN) model through initial comparative study of several popular CNN models. We then optimize the selected VGG19 model for the image modalities to show how the models can be used for the highly scarce and challenging COVID-19 datasets. We highlight the challenges (including dataset size and quality) in utilizing current publicly available COVID-19 datasets for developing useful deep learning models and how it adversely impacts the trainability of complex models. We also propose an image pre-processing stage to create a trustworthy image dataset for developing and testing the deep learning models. The new approach is aimed to reduce unwanted noise from the images so that deep learning models can focus on detecting diseases with speci c features from them. Our results indicate that Ultrasound images provide superior detection accuracy compared to X-Ray and CT scans. The experimental results highlight that with limited data, most of the deeper networks struggle to train well and provides less consistency over the three imaging modes we are using. The selected VGG19 model, which is then extensively tuned with appropriate parameters, performs in considerable levels of COVID-19 detection against pneumonia or normal for all three lung image modes with the precision of up to 86% for X-Ray, 100% for Ultrasound and 84% for CT scans.

INDEX TERMS COVID-19 detection, image processing, model comparison, CNN models, X-ray, ultrasound and CT based detection.

I. INTRODUCTION

The current COVID-19 pandemic has impacted the world with over 18.35 million infections and over 6,96,147 deaths so far (as of 5th August 2020) [1]. Early identifying, isolation and care for patients is a key strategy for a better management of this pandemic. Our study aims to provide a conceptual transfer learning framework to support COVID-19 detection with the use of image classi cation using deep learning models for multiple imaging modes including X-Ray, Ultrasound, and CT scan. The acquisition of a suf ciently large, publicly available corpus of medical image sample data for fully training deep learning models is challenging for novel medical conditions such as COVID-19 since collection and labelling of images requires signi cant time and resources to compile. An alternative method of training deep learning models is

The associate editor coordinating the review of this manuscript and approving it for publication was Derek Abbott.

``transfer learning'' whereby a deep learning network is pre-weighted with the results of a previous training cycle from a different domain. This technique is commonly used as a basis for initializing deep learning models which are then ne-tuned using the limited available medical sample data set with results that have been documented to outperform fully trained networks under certain circumstances [2], [3]. The study will demonstrate how transfer learning can be used for COVID-19 detection for three commonly used imaging modes X-Ray, Ultrasound, and CT scan. This could assist practitioners and researchers in developing a supporting tool for highly constrained health professionals in determining the course of treatment. The study further demonstrates a pre-processing pipeline for improving the image quality, for deep learning-based predictions. An initial testing is also conducted to understand the suitability of various popular deep learning models for the limited available dataset in order to select a model for the proposed image classi cation demonstrations on multiple image modes.

Fast, accessible, affordable and reliable identi cation of COVID-19 pathology in an individual is key to slowing the transmission of COVID-19 infection. Currently, reverse transcriptase quantitative polymerase chain reaction (RT-qPCR) tests are the gold standard for diagnosing COVID-19 [4]. During this test small amounts of viral RNA are extracted from a nasal swab, ampli ed, and quanti ed with virus detection indicated visually using a uorescent dye. Unfortunately, the RT-qPCR test is manual and time-consuming, with results taking up to two days. Some studies have also shown false positive Polymerase Chain Reaction PCR testing [5]. Other testing approaches include imaging technology-based approaches including computed tomography (CT) imaging [6] and X-Ray imaging based [7], [8] and Ultrasound imaging [9].

The CT scan-based COVID-19 detection is time consuming and manual with the requirement of expert involvements. CT scanning machines are also dif cult to use for COVID patients, as the patients often need to be transferred to the CT room, the machines would require extensive cleaning after each usage, and higher radiation risks [10]. Although CT is not recommended as a primary diagnostic tool, it has been successfully used as a supporting tool for COVID-19 condition assessment [6]. Common CT ndings include ground-glass opacities (GGO) at the early stage, during progressive stage, air space consolidation during peak stage, Broncho vascular thickening in the lesion, and traction bronchiectasis are visible during absorption stage [10]. Several studies have shown promising results in using deep learning models to automated diagnosis of COVID-19 from CT images [6], [11], [12]. Both the PCR tests and CT scans are comparatively costly [13], [14] and with an overwhelming demand many countries are forced to perform selective testing for only high-risk population.

X-Ray imaging is relatively cost effective and commonly utilized for lung infection detection and is useful for COVID-19 detection as well [15]. Medical observations were made by one of the co-authors of this research (Dr. Saha) who is also a medical professional, as well as by treating doctors of the COVID-19 dataset [16] patients. The common features observed in the X-Ray images of patients with COVID-19 are patchy in ltrates or opacities that bear similarities to other viral pneumonia features. X-Ray images do not show any abnormalities in the early stages of COVID-19. However, as the disease progresses, COVID-19 gradually manifests as a typical unilateral patchy in ltration involving mid zone and upper or lower zone of the lungs, occasionally with evidence of a consolidation.

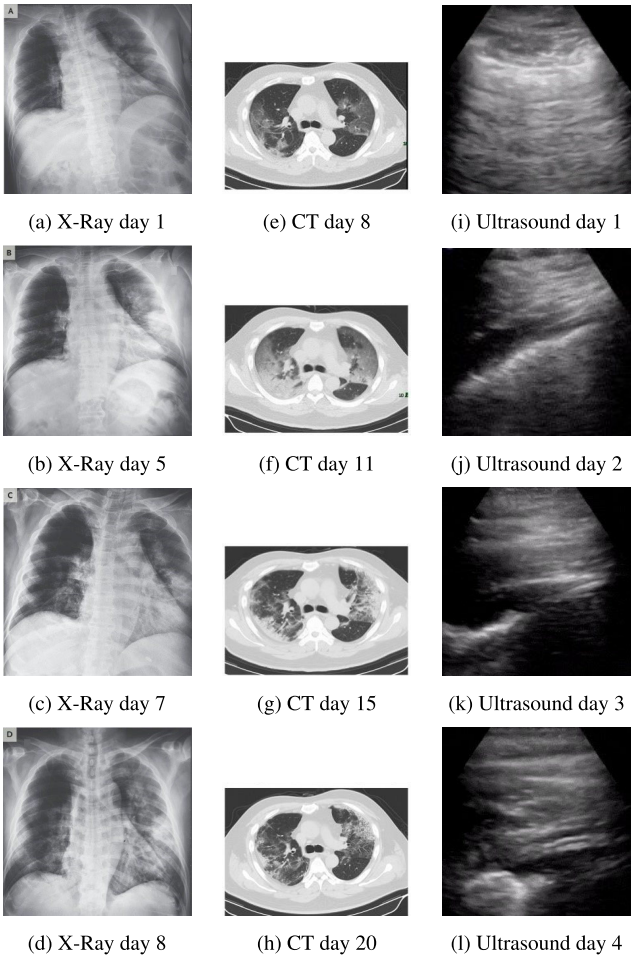

FIGURE 1. **COVID-19 progression over several days as evident in different imaging modes.**

Ultrasound imaging has also been recommended as a tool for COVID-19 lung condition assessment since it can be used at bedside with minimal infection spreading risks and has excellent ability to detect lung conditions related to COVID-19 [17]. Progression of COVID-19 infection is evident as B-lines aeration in early stages of consolidation in critical stages [10], [18].

Fig. 1 shows the progression of evidence for the patient in the COVID-19 datasets for X-Ray, CT and Ultrasound imaging.

Computer vision diagnostic tools for COVID-19 from multiple imaging modes such as X-Ray, Ultrasound, and CT would provide an automated ``second reading'' to clinicians, assisting in the diagnosis and criticality assessment of COVID-19 patients to assist in better decision making in the global fight against the disease. COVID-19 often results in pneumonia, and for radiologists and practitioners differentiating between the COVID-19 pneumonia and other types of pneumonia (viral and bacterial) solely based on diagnostic images could be challenging [19].

Deep learning artificial neural networks, and the Convolutional Neural Networks (CNNs) have proven to be highly effective in a vast range of medical image classification applications [20], [21]. In this study, we present three key contributions. Primarily, we demonstrate how transfer learning capabilities of off the shelf deep learning models can be utilized to perform classifications in two distinct scenarios for three imaging modes X-Ray, Ultrasound, and CT scan:

1) Identifying the pneumonia (both COVID-19 and other types) affected lung against the normal lung.
2) Identifying COVID-19 affected lung from non COVID-19 pneumonia affected lung.

Secondly, we present a comparative study in order to select a suitable deep learning model for our demonstration. We performed a comparative testing of several common off-the-shelf CNN models namely VGG16/VGG19 [22], Resnet50 [23], Inception V3 [24], Xception [25], InceptionResNet [26], DenseNet [27], and NASNetLarge [28]. The testing is not intended for exhaustive performance comparison of these methods, rather we wanted to select the most suitable one for our multi-modal image classification, which performs decently with minimal tuning. The source X-Ray, Ultrasound, and CT image samples, especially those from the COVID-19 data sets, have been harvested from multiple sources and are of inconsistent quality. In our final contribution, we have implemented a pre-processing pipeline to reduce unwanted signal noise such as non-lung area visible in X-Rays, and thereby reduce the impact of sampling bias on this comparison. Through this pre-processing pipeline, we minimize the image quality imbalances in the image samples. This would allow models to train on lung features only thus having a greater chance of learning disease features and ignoring other noise features. The study would provide timely model selection guidelines to the practitioners who often are resorted to utilise certain mode of imaging due to time and resource scarcity.

In the following sections we first present a brief review of recent scholarly works related to this study, followed by a discussion on the datasets we used and related challenges. We then present the dataset generation process along with our proposed pre-processing pipeline for data quality balancing. We then present the deep learning model selection process along with comparison results. Finally, we present the performance results with discussions for our selected model on all three image modes.

II. RELATED WORK

Computer aided detection and diagnosis of pulmonary pathologies from X-Ray images is a field of research that started in the 1960s and steadily progressed in the following decades with papers describing highly accurate diagnosis of a range of conditions including osteoporosis [29], breast cancer [30], and cardiac disease [31].

CT scans also use X-Rays as a radiation source, however, they provide much higher image resolution and contrast compared to standard X-Ray images because of a much more focused X-Ray beam used to produce cross-sectional images of the patient [32]. CT is generally considered as the best imaging modality for lung parenchyma and is widely accepted by clinicians as the ``gold standard'' [33]. A large corpus of research exists relating to the use of machine learning to improve the efficiency and accuracy of lung cancer diagnosis largely driven by extensive CT based lung cancer screening programs in many parts of the world. Several researches have achieved incredibly accurate results using CNNs with transfer learning to detect lung nodules [34] [37]. Recently a deep learning system built by Google achieved state-of-the-art performance using patients' current and prior CT volumes to predict the risk of lung cancer. This system outperformed human radiologists where prior CT scans were not available, and equaled human radiologist performance where historical CT scans were available [38]. Although X-Ray is the current reference diagnosis for pneumonia, some studies point out that CT generally outperforms X-Ray as a diagnostic tool for pneumonia, albeit at higher cost and convenience [39], [40].

Ultrasound has traditionally been used diagnostically in the fields of cardiology and obstetrics and more recently for a range of other conditions covering most organs. One of the reasons for this increase in the use of ultrasound is that technical advancements including machine learning have allowed useful information to be determined from the low quality and high signal-to-noise images that are typical of the Ultrasound imaging modality [41]. Several researchers have recently used Ultrasound as an effective diagnostic aid in hepatic steatosis, adenomyosis, and craniosynostosis [42], Pancreatic cancer [43], Breast cancer [44] and prostate cancer [45]. Use of bedside ultrasound in critically ill patients compared favorably against chest X-Ray and approached the diagnostic accuracy of CT scans for a range of thoracic conditions [46]. The combination of lung ultrasound with machine learning techniques was found to be valuable in providing faster and more accurate bedside interpretation of lung ultrasound for acute respiratory failure [47].

Difficulties in distinguishing soft tissue caused by poor contrast in X-Ray images have led some researchers to implement contrast enhancement [48] as a pre-processing step in X-Ray based diagnosis. In addition, lung segmentation of X-Ray images is an important step in the identification of lung nodules and various segmentation approaches are proposed in the literature based on linear filtering/thresholding, rolling ball filters and more recently CNNs [49].

Although CT scans are much higher contrast/resolution compared to X-Ray factors such as low dose and improper use of image enhancement can lead to poor quality images. A number of researchers have noted that histogram equalization techniques, particularly adaptive histogram equalization can improve the contrast of CT images [50]. A combination of histogram normalization, gamma correction and contrast limited adaptive histogram equalization has been shown to objectively improve the quality of poor contrast CT images [51].

Ultrasound images tend to be noisy due to the relatively low penetration of soundwaves into organic tissue compared to X-Rays. This limitation has led a number of researchers to develop methods to improve the quality of ultrasound images by various means including noise filtering, wavelet transformation and deconvolution [52]. Contrast Limited Adaptive Histogram Equalization (CLAHE) has been used as part of a pre-processing pipeline to enhance the quality of ultrasound images [53].

In the literature review we noted a small number of very recent studies that have used deep learning systems for COVID-19 screening and diagnosis. A custom-built 18-layer residual network pre-trained on the ImageNet weights against COVID-19 (100 images) and Pneumonia (1431 images) X-Ray image datasets [54]. A range of deep learning frameworks coined as COVIDX-Net trained on a small data set of 25 confirmed COVID-19 cases [55]. A custom curated dataset of COVID-19, viral pneumonia and normal X-Ray images [56]. A custom residual CNN that was highly effective in distinguishing between COVID-19, Pneumonia and normal condition X-Ray images [57]. These studies used the COVID-19 dataset [16] for the COVID-19 X-Ray samples, and the RSNA dataset [58] was used to get pneumonia and normal X-Ray samples.

Automated COVID-19 Pneumonia diagnosis from CT scans has been the focus of recent studies with promising results [59] [62]. A combined U-Net segmentation and 3D classification CNN has been used to accurately predict the presence of COVID-19 with an accuracy of 90% using a non-public dataset of CT images [63]. A ResNet50 based CNN with transfer learning from the ImageNet weights was able to classify COVID-19 with 94% accuracy [64] against a normal condition CT slice using unspecified multiple international datasets as a corpus. In a recent work, [65] addressed the challenge of automatically distinguishing between COVID-19 and community acquired pneumonia using machine learning. This system uses a U-Net pre-processor model for lung field segmentation, followed by a 3D ResNet50 model using transferred ImageNet weights. This study achieved a sensitivity of 87% against a large non-public dataset collected from 6 hospitals. The DenseNet-169 CNN has been used [66] to detect COVID-19 vs non-COVID-19 CT slices. Without segmentation this system achieved an accuracy of 79.5% with an F1 score of 76%. Using joint segmentation, the classification accuracy was raised to 83.3% with an F1 score of 84.6%.

There has been less attention given to the use of machine learning to automate COVID-19 diagnosis from Ultrasound images, however a ResNet based CNN trained on the available Ultrasound COVID-19 data has achieved an accuracy of 89% with recall accuracy for COVID-19 of 96% [9].

Each imaging mode differs in terms of cost/availability and the level of clinical expertise required to accurately interpret the generated medical images. Different imaging modes are therefore suitable to different contexts for example both X-Ray and Ultrasound can be implemented as low-cost portable units that may be used as bedside or even as field diagnostic tools. CT scanning equipment is typically physically fixed at high cost and is therefore only available within the confines of hospitals and medical clinics. Our main aim is to first select one suitable deep learning model through comparative testing of a range of off-the-shelf deep learning models against each of these imaging modes using transfer learning. The comparison results are then used to address limited sample data size and data variability. We then applied image pre-preprocessing to improve image quality and reduce inter and intra dataset systematic differences in brightness and contrast level. Finally, we performed extensive parameter tuning on the selected model and compared the performance of this model for each imaging mode.

III. DATASET DEVELOPMENT

A. DATA SOURCING

Large numbers of X-Ray, CT and Ultrasound images are available from several publicly accessible datasets. With the emergence of COVID-19 being very recent none of these large repositories contain any COVID-19 labelled data, thereby requiring that we rely upon multiple datasets for Normal, Pneumonia, COVID-19 and other non COVID-19 source images.

COVID-19 chest X-Rays were obtained from the publicly accessible COVID-19 Image Data Collection [16]. This collection has been sourced from websites and pdf format publications. Unsurprisingly, the images from this collection are of variable size and quality. Image contrast levels, brightness and subject positioning are all highly variable within this dataset. Our analysis in this article is based on a download of this dataset made on 11 May 2020.

The selection of a dataset for Normal and Pneumonia condition X-Rays posed a dilemma since a highly curated data set is not comparable to the available COVID-19 chest X-Ray dataset. Our early tests against one such dataset gave an unrealistically high classification accuracy for the quality of the data under test. We found that the National Institute of Health (NIH) Chest X-Ray [67] dataset provided images are of a similar size, [68] quality and aspect ratio to the typical images in the COVID-19 dataset with dimensions being uniformly 1024 1024 pixels in a portrait orientation.

CT scans for COVID-19 and non COVID-19 were obtained from the publicly accessible COVID-CT Dataset [66]. This dataset has been sourced by extracting CT slice images showing the COVID-19 pathology from preprint papers. Once again, the images from this collection are of variable size and

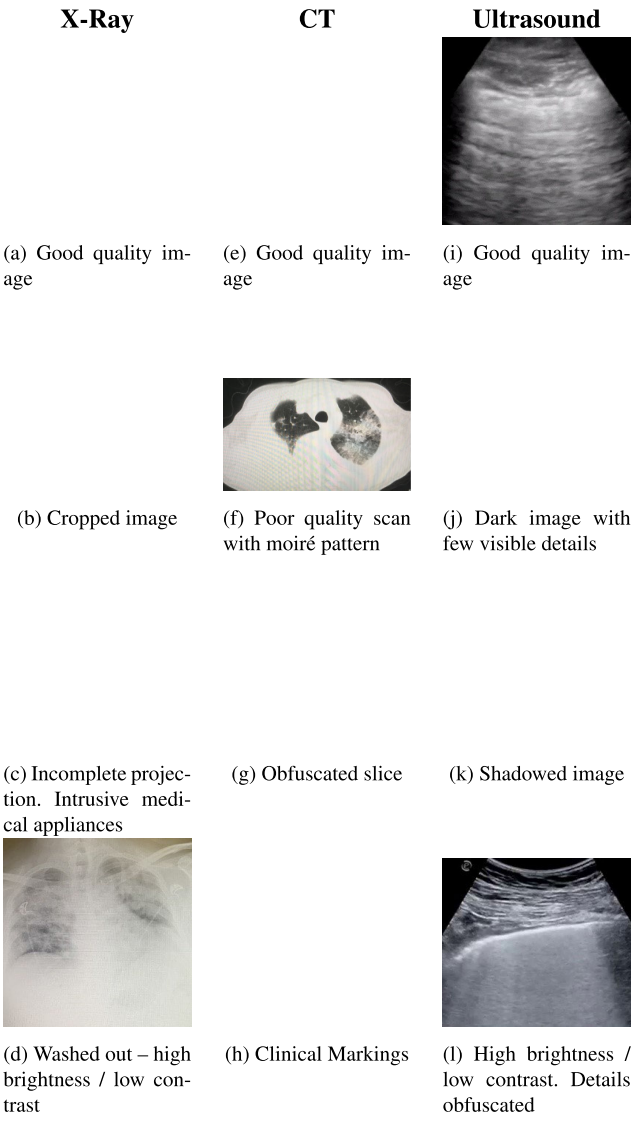

FIGURE 2. **Different variations observed in the COVID-19 datasets.**

quality. Moreover, the process of CT scanning is dynamic, with a full scan consisting of many discrete slices taken in a helical pattern along the thoracic cavity. The images in this collection only present a single, or small number of slices per patient. As CT slice images progress along the thoracic cavity, the structural features visible in the generated image change dramatically. Ideally all slices would be available for analysis in order to equalize the distribution/prominence in the image of these features, however this is not the case with this dataset. Our analysis in this article is based on a download of this dataset made on 11 May 2020.

Ultrasound images for COVID-19, Pneumonia and Normal conditions were obtained from the publicly accessible POCOVID-Net data set [9]. These images have been sampled from video sourced from various online sources. We noticed a huge variation in the quality in the images within each condition caused by the position of the ultrasound apparatus on the patients' chest. Ideally ultrasound video would be taken in a systematic way to allow for greater comparability of the condition datasets with every frame in the video subject to analysis. Neither of these conditions are satis ed by this dataset. Our analysis in this article is based on a download of this dataset made on 11 May 2020.

TABLE 1. **Summary of data sources used.**

Collection	Number of Images	Characteristics	Notes
COVID-19 Image Data Collection [16]	115: COVID-19 (PA)	Variable size, quality, contrast and brightness.	Only source of publicly accessible COVID-19 PA X-Ray images and used in this study.
NIH Chest X-Ray [67]	322: Pneumonia 60361: No Finding	Intra-dataset uniformity similar to COVID-19 dataset. All images are 1024 x1024 in size.	Objectively similar in quality to the COVID-19 Image Data Collection. Used in this study.
COVID-CT Dataset [66]	349: COVID-19 397: Non COVID	Variable size, contrast and brightness	Only source of publicly accessible COVID-19 CT images and used in this study.
POCOVID-Net Dataset [9]	654: COVID-19 277: Pneumonia 172: No Finding	Variable size, contrast and brightness	Only source of publicly accessible COVID-19 Ultrasound images and used in this study.

The number of images of each dataset along with a description of the characteristics of the datasets is described in Table 1. We believe the signi cant quality variations between data from different classes need to be balanced for deep learning models to learn actual disease related variations. Therefore, our study stresses the importance of sampling bias/signal noise removal from the image datasets prior to using them for model development and classi cation in order to obtain meaningful and trustworthy classi cation results. Some illustrative examples of this variability of these datasets is shown in Fig. 2. Of these examples images (b), (c) and (f) appear to have been cropped from journal articles and in the case of (f) scanned. These images are of poor quality and lacking detail that would indicate a pathology to our machine learning models. Images (g), (j) and (k) also lack detail as a result of apparatus positioning. Images (d) and (l) show high brightness and low contrast, thus hiding pathological details. Despite the variability of the datasets we chose to only very lightly curate data as described in Section III (C) Data Pre-processing and shown in Table 2. Our reasoning for this is twofold. Firstly we wish to avoid biasing the data corpus with a non-expert subjective opinion of pathological indications, and secondly we consider the usefulness of this study to potentially extend to future pandemic situations where similar data quality issues will be likely if not inevitable.

TABLE 4. **Datasets used for experiments.**

Exp ID	Image Mode	Experiment	Dataset
1A	X-Ray	Normal vs (COVID-19 and Pneumonia)	(400 x Normal) vs (190 x Pneumonia 139 x COVID-19)
1B	Ultrasound	Normal vs (COVID-19 and Pneumonia)	226 x Normal vs (235 x COVID-19 220 x Pneumonia)
2A	X-Ray	COVID-19 vs Pneumonia	139 x COVID-19 vs 190 x Pneumonia
2B	Ultrasound	COVID-19 vs Pneumonia	235 x COVID-19 vs 220 x Pneumonia
3A	CT	COVID-19 vs Non COVID	349 x COVID-19 vs 397 x Non COVID

of 10 ^{4} and 10 ^{5} provided higher model accuracy with 10 ^{5} achieving more consistent results. There is a tendency for accuracy to improve with batch size increase at learning rates of 10 ^{3} and 10 ^{6} but at learning rates of 10 ^{4} and 10 ^{5} this tendency is not apparent. Finally, there is also a trend towards higher accuracy with a larger hidden layer size that is most noticeable at 10 ^{3}. Taking a learning rate of 10 ^{5} as achieving consistent high accuracy, we can then suggest from this analysis that a hidden layer size ranging from 64 to 96 and batch size of 4 could generally be expected to provide the most accurate results for this experiment. Through similar analysis for each experiment in Table 4, we have identi ed the best parameter settings for each experiment as shown in Table 5.

The results of the ve experiments are listed in Table 5. For experiments classifying COVID-19 and Pneumonia vs Normal (1A and 2A) we found that the Ultrasound mode provided the best results with a sensitivity of 97% and positive predictive value of 99% compared to X-Ray with 83% and 85% respectively. For experiments classifying COVID-19 vs Pneumonia (1B and 2B) we again found that the Ultrasound mode provided the best results with a sensitivity of 100% and a positive predictive value of 100% compared to X-Ray with sensitivity of 86% and positive predictive value of 86%. The CT imaging mode was found to have a sensitivity of 83% and positive predictive value of 79% in classifying COVID-19 vs non COVID-19 scans. All experiments resulted in F1 scores exceeding 80% which is a good result given the relatively small and variable quality data corpus available.

The learning curves for each experiment are shown in Fig. 7. The training curves for both Ultrasound experiments (2A and 2B) are close to ideal. The training curves for the X-Ray experiments (1A and 2A) are also very good, although the curve for experiment 1B does show some signs

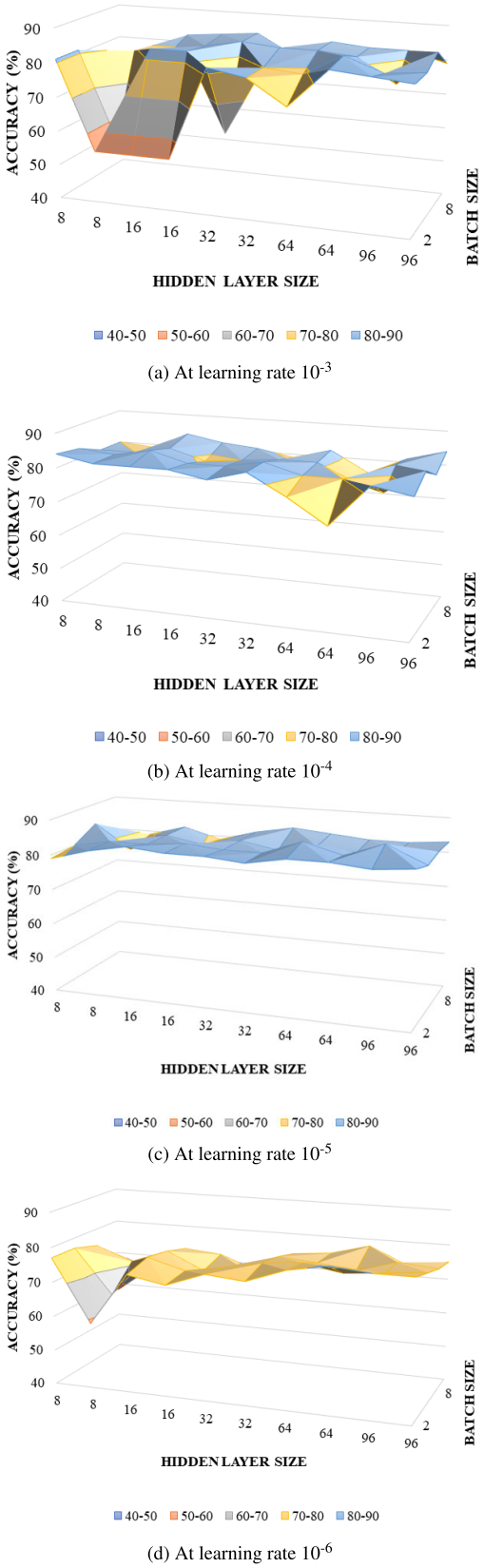

FIGURE 6. **Model sensitivity to hyperparameters for experiment 1A.**

TABLE 5. **Experiment results for three image modes.**

Image mode	Experiment	Parameters	Classification	Results
X-Ray	1A	LR: 10^{-5} DR: 0.1 BS: 4 HS: 64 Epochs: 100	COVID-19 + Pneumonia	P: 0.85 R: 0.83 F1: 0.84
			Normal	P: 0.86 R: 0.88 F1: 0.87
Ultrasound	2A	LR: 10^{-5} DR: 0.2 BS: 2 HS: 64 Epochs: 100	COVID-19 + Pneumonia	P: 0.99 R: 0.97 F1: 0.98
			Normal	P: 0.94 R: 0.98 F1: 0.96
X-Ray	1B	LR: 10^{-3} DR: 0.2 BS: 8 HS: 8 Epochs: 100	COVID-19	P: 0.86 R: 0.86 F1: 0.86
			Pneumonia	P: 0.89 R: 0.89 F1: 0.89
Ultrasound	2B	LR: 10^{-5} DR: 0.2 BS: 2 HS: 64 Epochs: 100	COVID-19	P: 1.00 R: 1.00 F1: 1.00
			Pneumonia	P: 1.00 R: 1.00 F1: 1,00
CT	3A	LR: 10^{-3} DR: 0.2 BS: 4 HS: 16 Epochs: 70	COVID-19	P: 0.79 R: 0.83 F1: 0.81
			Non COVID	P: 0.84 R: 0.81 F1: 0.83

of erratic learning patterns, which is the expected result of the highly variable image quality in the COVID-19 data set. The learning curve for the CT mode experiment (3A) is very erratic even though the model did train, over tting is arguably apparent after the epoch 50. Once again this is the expected result considering signi cant variation in the CT image data sets.

The confusion matrices in Fig. 8 provides an indication of the false-negative and false-positive results of our experiments. Minimization of false negative predictions is important in the medical context since false reassurance may lead to diagnostic and treatment delay resulting in poor medical outcomes, patient mental distress, community loss in con - dence relating to medical services and legal consequences [96]. False negative predictions for the Ultrasound mode experiments were very low at 1 and 0 for experiments 2A and 2B, respectively. False negative predictions for the X-Ray mode experiments were higher with 11 and 4 for experiments 1A and 1B respectively. The CT mode (experiment 3A) also performed poorly in this respect with 12 false negatives. Once again, the limited sample size and variable quality of the COVID-19 data sets used for the X-Ray and CT experiments are the most likely cause of the relatively high number of false negatives for experiments 1A, 1B and 3A.

As previously noted, false negatives generated by the Keras class prediction threshold of 0.5 were high in the case of the

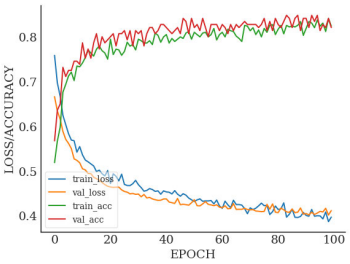

a) X-Ray Experiment 1A

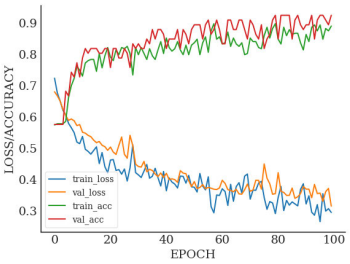

b) X-Ray Experiment 1B

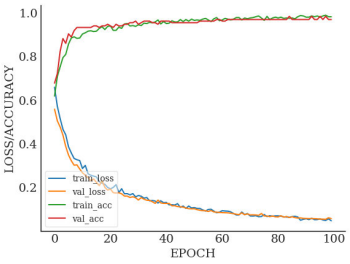

c) Ultrasound Experiment 2A

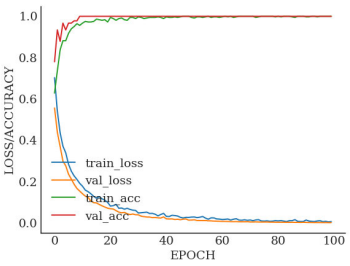

d) Ultrasound Experiment 2B

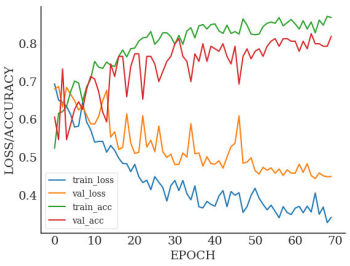

e) CT Experiment 3A

FIGURE 7. **Learning curves for different modes.**

CT and X-Ray imaging modes. We then performed adjustments in the class prediction threshold in 5% increments

to develop suitable deep learning-based tools for COVID-19 detection. The model is capable of classifying both Pneumonia vs Normal and COVID-19 vs Pneumonia conditions for multiple imaging modes including X-Ray, Ultrasound, and CT scan.

With very little data curation, we achieved considerable classi cation results using VGG19 from all imaging modes. Perhaps the most interesting observation is that the pre-trained models tuned very effectively for the Ultrasound image samples, which to the untrained eye appeared noisy and dif cult to interpret. Both training curves and confusion matrix for both Ultrasound experiments are close to ideal. VGG19 also trained well against the X-Ray image corpus however, without modi ed thresholding we found that the proportion of false negatives was concerning but not unexpected given data quality challenges. Our nding that experiment 1A/2A yielded lower F1 scores and higher false negatives than experiments 1B/2B was unexpected since the manifestation of COVID-19 is itself a form of viral pneumonia. This may indicate that despite our attempts to remove sampling bias using N-CLAHE pre-processing there may still be systematic differences in the COVID-19 image data sets that leads the VGG19 classi er to more easily distinguish the COVID-19 images from the pneumonia images. A future research direction could be to isolate the lung eld by segmentation for all image samples in order to remove noise and further reduce sampling bias. Our lower results against the CT image corpus were not surprising since the CT image slices available were not from a uniform patient location and displayed extremely high variability in both form and content.

Our study uncovers the challenging characteristics of the limited COVID-19 image datasets. This should be helpful for practitioners aiming to use these datasets for their research and development. We provided a pre-processing pipeline aimed to remove the sampling bias and improve image quality. Our preprocessed images are also made openly available for others to use. During our initial model selection experiment, we also found that both VGG16 and VGG19 classi ers provided good results within the experimental constraints of the small number of currently available COVID-19 medical images. While deeper networks generally struggled, they will perform better when larger datasets are available which will reduce the impact of data quality variation.

It is inevitable that the initial publicly available medical images for novel medical conditions such as COVID-19 will be low in number and poor in quality. In this situation we conclude that the VGG19 classi er with transfer learning provides a fast and simple to implement machine learning model for multiple imaging modes providing good results that may lead to clinically useful diagnostic tools.

Despite our promising results, we would urge great caution in the development of clinical diagnostic models using currently available COVID-19 image dataset. The effect of a false positive diagnosis of COVID-19 on an individual is the isolation of the individual and their contract traces and the mental anguish and stress caused by both the prognosis and the social isolation. A false positive COVID-19 diagnosis could result in an inappropriate course of treatment. The effects of a false negative COVID-19 diagnosis would also be devastating for the individual if that diagnosis led to an inappropriate lack of treatment, and also for the community since cautions against COVID-19 transmission may not be appropriately applied resulting in the further community spread of the disease.

As a higher quality corpus of COVID-19 diagnostic image data becomes available, it may be possible to produce clinically trusted deep learning-based models for the fast diagnosis of COVID-19 as distinguished from similar conditions such as pneumonia. Such a tool would prove invaluable in practice, where other diagnostic tests for COVID-19 are either unavailable or unreliable. As the COVID-19 spread progresses throughout remote and economically challenged locations, an ability to diagnose COVID-19 from a readily available and portable medical imaging equipment such as X-Ray and Ultrasound machines would help slow the spread of the disease and result in a better medical outcome for the population.

Data fusion concept allows us to combine multiple modes of data to improve model classi cation performance. Although data fusion comes with its own set of challenges [97], [98], it has been used successfully in other application areas such as remote sensing [99] [101], action detection [102], and medical diagnosis and imaging [103], [104]. We plan to extend our study with multimodal data fusion when suf cient data is available.

ACKNOWLEDGMENT

Michael J. Horry would like to thank IBM Australia for providing work time release to perform modelling and experimentation work and to contribute to the writing of this article.

REFERENCES

[1] (2020). *Who COVID-19 Situation Reports*. [Online]. Available: https://www.who.int/emergencies/diseases/novel-coronavirus-2019/situation-reports

[2] H. Ravishankar, P. Sudhakar, R. Venkataramani, S. Thiruvenkadam, P. Annangi, N. Babu, and V. Vaidya, ``Understanding the mechanisms of deep transfer learning for medical images,'' in *Deep Learning and Data Labeling for Medical Applications* (Lecture Notes in Computer Science), vol. 10008, G. Carneiro, Ed. Cham, Switzerland: Springer, 2016, pp. 188 196, doi: 10.1007/978-3-319-46976-820.

[3] Y. Yu, H. Lin, J. Meng, X. Wei, H. Guo, and Z. Zhao, ``Deep transfer learning for modality classi cation of medical images,'' *Information*, vol. 8, no. 3, p. 91, Jul. 2017, doi: 10.3390/info8030091.

[4] W. Wang, Y. Xu, R. Gao, R. Lu, K. Han, G. Wu, and W. Tan, ``Detection of SARS-CoV-2 in different types of clinical specimens,'' *JAMA*, vol. 323, pp. 1843 1844, Mar. 2020, doi: 10.1001/jama.2020.3786.

[5] C. Chen, G. Gao, Y. Xu, L. Pu, Q. Wang, L. Wang, W. Wang, Y. Song, M. Chen, L. Wang, F. Yu, S. Yang, Y. Tang, L. Zhao, H. Wang, Y. Wang, H. Zeng, and F. Zhang, ``SARS-CoV-2 positive sputum and feces after conversion of pharyngeal samples in patients with COVID-19,'' *Ann. Internal Med.*, vol. 172, no. 12, pp. 832 834, Jun. 2020, doi: 10.7326/M20-0991.

[6] T. Ai, Z. Yang, H. Hou, C. Zhan, C. Chen, W. Lv, Q. Tao, Z. Sun, and L. Xia, ``Correlation of chest CT and RT-PCR testing for coronavirus disease 2019 (COVID-19) in China: A report of 1014 cases,'' *Radiology*, vol. 296, no. 2, pp. E32 E40, Aug. 2020, doi: 10.1148/radiol.2020200642.

[7] M. Hosseiny, S. Kooraki, A. Gholamrezanezhad, S. Reddy, and L. Myers, ``Radiology perspective of coronavirus disease 2019 (COVID-19): Lessons from severe acute respiratory syndrome and middle east respiratory syndrome,'' *Amer. J. Roentgenology*, vol. 214, no. 5, pp. 1078 1082, May 2020, doi: 10.2214/AJR.20.22969.

[8] A. Ulhaq, A. Khan, D. Gomes, and M. Paul, ``Computer vision for COVID-19 control: A survey,'' 2020, *arXiv:2004.09420*. [Online]. Available: http://arxiv.org/abs/2004.09420

[9] J. Born, G. Brändle, M. Cossio, M. Disdier, J. Goulet, J. Roulin, and N. Wiedemann, ``POCOVID-net: Automatic detection of COVID-19 from a new lung ultrasound imaging dataset (POCUS),'' 2020, *arXiv:2004.12084*. [Online]. Available: http://arxiv.org/abs/2004.12084

[10] D. J. Bell. (2020). *COVID-19 Radiopaedia*. [Online]. Available: https://radiopaedia.org/articles/covid-19-4?lang=us

[11] J. Chen, L. Wu, J. Zhang, L. Zhang, D. Gong, Y. Zhao, S. Hu, Y. Wang, X. Hu, B. Zheng, K. Zhang, H. Wu, Z. Dong, Y. Xu, Y. Zhu, X. Chen, L. Yu, and H. Yu. (2020). *Deep Learning-Based Model for Detecting 2019 Novel Coronavirus Pneumonia on High-Resolution Computed Tomography: A Prospective Study*. [Online]. Available: https://medRxiv:2020.02.25.20021568

[12] S. Wang, B. Kang, J. Ma, X. Zeng, M. Xiao, J. Guo, M. Cai, J. Yang, Y. Li, X. Meng, and B. Xu. (2020). *A Deep Learning Algorithm Using CT Images to Screen for Corona Virus Disease (COVID-19)*. [Online]. Available: https://medRxiv:2020.02.14.20023028

[13] E. Livingston, A. Desai, and M. Berkwits, ``Sourcing personal protective equipment during the COVID-19 pandemic,'' *JAMA*, vol. 323, no. 19, pp. 1912 1914, 2020, doi: 0.1001/jama.2020.5317.

[14] L. J. M. Kroft, L. van der Velden, I. H. Girón, J. J. H. Roelofs, A. de Roos, and J. Geleijns, ``Added value of ultra low-dose computed tomography, dose equivalent to chest X-ray radiography, for diagnosing chest pathology,'' *J. Thoracic Imag.*, vol. 34, no. 3, pp. 179 186, May 2019, doi: 10.1097/RTI.0000000000000404.

[15] H. Y. F. Wong, H. Y. S. Lam, A. H.-T. Fong, S. T. Leung, T. W.-Y. Chin, C. S. Y. Lo, M. M.-S. Lui, J. C. Y. Lee, K. W.-H. Chiu, T. W.-H. Chung, E. Y. P. Lee, E. Y. F. Wan, I. F. N. Hung, T. P. W. Lam, M. D. Kuo, and M.-Y. Ng, ``Frequency and distribution of chest radiographic ndings in patients positive for COVID-19,'' *Radiology*, vol. 296, no. 2, pp. E72 E78, Aug. 2020, doi: 10.1148/radiol.2020201160.

[16] J. P. Cohen, P. Morrison, L. Dao, K. Roth, T. Q. Duong, and M. Ghassemi, ``COVID-19 image data collection: Prospective predictions are the future,'' 2020, *arXiv:2006.11988*. [Online]. Available: http://arxiv.org/abs/2006.11988

[17] D. Buonsenso, D. Pata, and A. Chiaretti, ``COVID-19 outbreak: Less stethoscope, more ultrasound,'' *Lancet Respiratory Med.*, vol. 8, no. 5, 2020, Art no. E27 doi: 10.1016/S2213-2600(20)30120-X.

[18] M. J. Smith, S. A. Hayward, S. M. Innes, and A. S. C. Miller, ``Point-of-care lung ultrasound in patients with COVID-19 A narrative review,'' *Anaesthesia*, vol. 75, no. 8, pp. 1096 1104, Aug. 2020, doi: 10.1111/anae.15082.

[19] (2020). *ACR Recommendations*. [Online]. Available: https://www.acr.org/Advocacy-and-Economics/ACR-Position-Statements/Recommendations-for -Chest-Radiography-and-CT-for-Suspected-COVID19-Infection

[20] R. Yamashita, M. Nishio, R. K. G. Do, and K. Togashi, ``Convolutional neural networks: An overview and application in radiology,'' *Insights into Imag.*, vol. 9, no. 4, pp. 611 629, Aug. 2018, doi: 10.1007/s13244-018-0639-9.

[21] M. A. Mazurowski, M. Buda, A. Saha, and M. R. Bashir, ``Deep learning in radiology: An overview of the concepts and a survey of the state of the art with focus on MRI,'' *J. Magn. Reson. Imag.*, vol. 49, no. 4, pp. 939 954, Apr. 2019, doi: 10.1002/jmri.26534.

[22] K. Simonyan and A. Zisserman, ``Very deep convolutional networks for large-scale image recognition,'' 2014, *arXiv:1409.1556*. [Online]. Available: http://arxiv.org/abs/1409.1556

[23] K. He, X. Zhang, S. Ren, and J. Sun, ``Deep residual learning for image recognition,'' in *Proc. IEEE Conf. Comput. Vis. Pattern Recognit. (CVPR)*, Las Vegas, NV, USA, Jun. 2016, pp. 770 778, doi: 10.1109/CVPR.2016.90.

[24] C. Szegedy, V. Vanhoucke, S. Ioffe, J. Shlens, and Z. Wojna, ``Rethinking the inception architecture for computer vision,'' in *Proc. IEEE Conf. Comput. Vis. Pattern Recognit. (CVPR)*, Las Vegas, NV, USA, Jun. 2016, pp. 2818 2826, doi: 10.1109/CVPR.2016.308.

[25] F. Chollet, ``Xception: Deep learning with depthwise separable convolutions,'' in *Proc. IEEE Conf. Comput. Vis. Pattern Recognit. (CVPR)*, Honolulu, HI, USA, Jul. 2017, pp. 1800 1807, doi: 10.1109/CVPR.2017.195.

[26] C. Szegedy, S. Ioffe, V. Vanhoucke, and A. Alemi, ``Inception-v4, inception-resnet and the impact of residual connections on learning,'' in *Proc. AAAI Conf. Artif. Intell.*, San Francisco, CA, USA: AAAI Press, 2017, pp. 4278 4284, doi: 10.5555/3298023.3298188.

[27] G. Huang, Z. Liu, L. Van Der Maaten, and K. Q. Weinberger, ``Densely connected convolutional networks,'' in *Proc. IEEE Conf. Comput. Vis. Pattern Recognit. (CVPR)*, Honolulu, HI, USA, Jul. 2017, pp. 2261 2269, doi: 10.1109/CVPR.2017.243.

[28] B. Zoph, V. Vasudevan, J. Shlens, and Q. V. Le, ``Learning transferable architectures for scalable image recognition,'' in *Proc. IEEE/CVF Conf. Comput. Vis. Pattern Recognit.*, Salt Lake City, UT, USA, Jun. 2018, pp. 8697 8710, doi: 10.1109/CVPR.2018.00907.

[29] P. Pisani, M. D. Renna, F. Conversano, E. Casciaro, M. Muratore, E. Quarta, M. D. Paola, and S. Casciaro, ``Screening and early diagnosis of osteoporosis through X-ray and ultrasound based techniques,'' *World J. Radiol.*, vol. 5, no. 11, pp. 398 410, 2013, doi: 10.4329/wjr.v5.i11.398.

[30] M. A. Al-antari, M. A. Al-masni, M.-T. Choi, S.-M. Han, and T.-S. Kim, ``A fully integrated computer-aided diagnosis system for digital X-ray mammograms via deep learning detection, segmentation, and classi cation,'' *Int. J. Med. Informat.*, vol. 117, pp. 44 54, Sep. 2018, doi: 10.1016/j.ijmedinf.2018.06.003.

[31] M. A. Speidel, B. P. Wil ey, J. M. Star-Lack, J. A. Heanue, and M. S. Van Lysel, ``Scanning-beam digital X-ray (SBDX) technology for interventional and diagnostic cardiac angiography,'' *Med. Phys.*, vol. 33, no. 8, pp. 2714 2727, Jul. 2006, doi: 10.1118/1.2208736.

[32] A. C. Mamourian, *CT Imaging: Practical Physics, Artifacts, and Pitfalls*. New York, NY, USA: Oxford Univ. Press, 2013.

[33] J. A. Verschakelen and W. de Wever, *Computed Tomography of the Lung: A Pattern Approach* (Medical Radiology), 2nd ed. Berlin, Germany: Springer-Verlag, 2018.

[34] T. Sajja, R. Devarapalli, and H. Kalluri, ``Lung cancer detection based on CT scan images by using deep transfer learning,'' *Traitement du Signal*, vol. 36, no. 4, pp. 339 344, Oct. 2019, doi: 10.18280/ts.360406.

[35] W. Shen, M. Zhou, F. Yang, C. Yang, and J. Tian, ``Multi-scale convolutional neural networks for lung nodule classi cation,'' in *Information Processing in Medical Imaging* (Lecture Notes in Computer Science), vol. 9123, S. Ourselin, D. Alexander, C. Westin, and M. Cardoso, Eds. Cham, Switzerland: Springer, 2015, pp. 588 599, doi: 10.1007/978-3-319-19992-4_46.

[36] W. Sun, B. Zheng, and W. Qian, ``Automatic feature learning using multichannel ROI based on deep structured algorithms for computerized lung cancer diagnosis,'' *Comput. Biol. Med.*, vol. 89, pp. 530 539, Oct. 2017, doi: 10.1016/j.compbiomed.2017.04.006.

[37] A. Masood, P. Yang, B. Sheng, H. Li, P. Li, J. Qin, V. Lanfranchi, J. Kim, and D. D. Feng, ``Cloud-based automated clinical decision support system for detection and diagnosis of lung cancer in chest CT,'' *IEEE J. Transl. Eng. Health Med.*, vol. 8, Dec. 2020, Art. no. 4300113, doi: 10.1109/JTEHM.2019.2955458.

[38] D. Ardila, A. P. Kiraly, S. Bharadwaj, B. Choi, J. J. Reicher, L. Peng, D. Tse, M. Etemadi, W. Ye, G. Corrado, D. P. Naidich, and S. Shetty, ``End-to-end lung cancer screening with three-dimensional deep learning on low-dose chest computed tomography,'' *Nature Med.*, vol. 25, no. 6, pp. 954 961, Jun. 2019, doi: 10.1038/s41591-019-0447-x.

[39] N. Garin, C. Marti, S. Carballo, P. D. Farhoumand, X. Montet, X. Roux, M. Schef er, C. Serratrice, J. Serratrice, Y.-E. Claessens, X. Duval, P. Loubet, J. Stirnemann, and V. Prendki, ``Rational use of CT-scan for the diagnosis of pneumonia: Comparative accuracy of different strategies,'' *J. Clin. Med.*, vol. 8, no. 4, p. 514, Apr. 2019, doi: 10.3390/jcm8040514.

[40] W. H. Self, D. M. Courtney, C. D. McNaughton, R. G. Wunderink, and J. A. Kline, ``High discordance of chest X-ray and computed tomography for detection of pulmonary opacities in ED patients: Implications for diagnosing pneumonia,'' *Amer. J. Emergency Med.*, vol. 31, no. 2, pp. 401 405, Feb. 2013, doi: 10.1016/j.ajem.2012.08.041.

[41] J. M. Sanches, A. Laine, and J. S. Suri, *Ultrasound Imaging: Advances and Applications*. New York, NY, USA: Springer, 2012.

[42] J. Y. Wu, A. Tuomi, M. D. Beland, J. Konrad, D. Glidden, D. Grand, and D. Merck, ``Quantitative analysis of ultrasound images for computer-aided diagnosis,'' *J. Med. Imag.*, vol. 3, no. 1, Jan. 2016, Art. no. 014501, doi: 10.1117/1.jmi.3.1.014501.

[43] M. Zhu, C. Xu, J. Yu, Y. Wu, C. Li, M. Zhang, Z. Jin, and Z. Li, ``Differentiation of pancreatic cancer and chronic pancreatitis using computer-aided diagnosis of endoscopic ultrasound (EUS) images: A diagnostic test,'' *PLoS ONE*, vol. 8, no. 5, May 2013, Art. no. e63820, doi: 10.1371/journal.pone.0063820.

[44] Y. Wang, H. Wang, Y. Guo, C. Ning, B. Liu, H. D. Cheng, and J. Tian, ``Novel computer-aided diagnosis algorithms on ultrasound image: Effects on solid breast masses discrimination,'' *J. Digit. Imag.*, vol. 23, no. 5, pp. 581 591, Oct. 2010, doi: 10.1007/s10278-009-9245-1.

[45] A. E. Hassanien, H. Al-Qaheri, V. Snasel, and J. F. Peters, ``Machine learning techniques for prostate ultrasound image diagnosis,'' in *Advances in Machine Learning I* (Studies in Computational Intelligence), vol. 262, J. Koronacki, Z. W. Ras, S. T. Wierzchon, and J. Kacprzyk, Eds. Berlin, Germany: Springer, 2010, pp. 385 403, doi: 10.1007/978-3-642-05177-719.

[46] N. Xirouchaki, E. Magkanas, K. Vaporidi, E. Kondili, M. Plataki, A. Patrianakos, E. Akoumianaki, and D. Georgopoulos, ``Lung ultrasound in critically ill patients: Comparison with bedside chest radiography,'' *Intensive Care Med.*, vol. 37, no. 9, pp. 1488 1493, Sep. 2011, doi: 10.1007/s00134-011-2317-y.

[47] B. Bataille, B. Riu, F. Ferre, P. E. Moussot, A. Mari, E. Brunel, J. Ruiz, M. Mora, O. Fourcade, M. Genestal, and S. Silva, ``Integrated use of bedside lung ultrasound and echocardiography in acute respiratory failure,'' *Chest*, vol. 146, no. 6, pp. 1586 1593, Dec. 2014.

[48] N. Kanwal, A. Girdhar, and S. Gupta, ``Region based adaptive contrast enhancement of medical X-ray images,'' in *Proc. 5th Int. Conf. Bioinf. Biomed. Eng.*, May 2011, pp. 1 5, doi: 10.1109/icbbe.2011.5780221.

[49] M. R. Arbabshirani, A. H. Dallal, C. Agarwal, A. Patel, and G. Moore, ``Accurate segmentation of lung elds on chest radiographs using deep convolutional networks,'' *Proc. SPIE*, vol. 10133, Feb. 2017, Art. no. 1013305, doi: 10.1117/12.2254526.

[50] A.-A. Zohair, A.-A. Shamil, and S. Ghazali, ``Latest methods of image enhancement and restoration for computed tomography: A concise review,'' *Appl. Med. Inform.*, vol. 36, no. 1, pp. 1 12, 2015.

[51] Z. Al-Ameen, G. Sulong, A. Rehman, A. Al-Dhelaan, T. Saba, and M. Al-Rodhaan, ``An innovative technique for contrast enhancement of computed tomography images using normalized gamma-corrected contrast-limited adaptive histogram equalization,'' *EURASIP J. Adv. Signal Process.*, vol. 2015, no. 1, pp. 1 12, Dec. 2015, doi: 10.1186/s13634-015-0214-1.

[52] S. H. Contreras Ortiz, T. Chiu, and M. D. Fox, ``Ultrasound image enhancement: A review,'' *Biomed. Signal Process. Control*, vol. 7, no. 5, pp. 419 428, Sep. 2012, doi: 10.1016/j.bspc.2012.02.002.

[53] P. Singh, R. Mukundan, and R. De Ryke, ``Feature enhancement in medical ultrasound videos using contrast-limited adaptive histogram equalization,'' *J. Digit. Imag.*, vol. 33, no. 1, pp. 273 285, Feb. 2020, doi: 10.1007/s10278-019-00211-5.

[54] J. Zhang, Y. Xie, Z. Liao, G. Pang, J. Verjans, W. Li, Z. Sun, J. He, Y. Li, C. Shen, and Y. Xia, ``COVID-19 screening on chest X-ray images using deep learning based anomaly detection,'' 2020, *arXiv:2003.12338*. [Online]. Available: http://arxiv.org/abs/2003.12338

[55] E. El-Din Hemdan, M. A. Shouman, and M. Esmail Karar, ``COVIDX-net: A framework of deep learning classi ers to diagnose COVID-19 in X-ray images,'' 2020, *arXiv:2003.11055*. [Online]. Available: http://arxiv.org/abs/2003.11055

[56] M. E. H. Chowdhury, T. Rahman, A. Khandakar, R. Mazhar, M. Abdul Kadir, Z. Bin Mahbub, K. Reajul Islam, M. Salman Khan, A. Iqbal, N. Al-Emadi, M. B. I. Reaz, and T. I. Islam, ``Can AI help in screening viral and COVID-19 pneumonia?'' 2020, *arXiv:2003.13145*. [Online]. Available: http://arxiv.org/abs/2003.13145

[57] L. Wang and A. Wong, ``COVID-net: A tailored deep convolutional neural network design for detection of COVID-19 cases from chest X-ray images,'' 2020, *arXiv:2003.09871*. [Online]. Available: http://arxiv.org/abs/2003.09871

[58] (2020). *RSNA Challenge*. [Online]. Available: https://www.kaggle.com/c/rsna-pneumonia-detection-challenge

[59] M. Polsinelli, L. Cinque, and G. Placidi, ``A light CNN for detecting COVID-19 from CT scans of the chest,'' 2020, *arXiv:2004.12837*. [Online]. Available: http://arxiv.org/abs/2004.12837

[60] D. Singh, V. Kumar, K. Vaishali, and M. Kaur, ``Classi cation of COVID-19 patients from chest CT images using multi-objective differential evolution based convolutional neural networks,'' *Eur. J. Clin. Microbiology Infectious Diseases*, vol. 39, no. 7, pp. 1379 1389, Jul. 2020, doi: 10.1007/s10096-020-03901-z.

[61] X. Ouyang, J. Huo, L. Xia, F. Shan, J. Liu, Z. Mo, F. Yan, Z. Ding, Q. Yang, B. Song, F. Shi, H. Yuan, Y. Wei, X. Cao, Y. Gao, D. Wu, Q. Wang, and D. Shen, ``Dual-sampling attention network for diagnosis of COVID-19 from community acquired pneumonia,'' *IEEE Trans. Med. Imag.*, vol. 39, no. 8, pp. 2595 2605, Aug. 2020, doi: 10.1109/TMI.2020.2995508.

[62] H. S. Maghdid, A. T. Asaad, K. Z. Ghafoor, A. S. Sadiq, and M. K. Khan, ``Diagnosing COVID-19 pneumonia from X-ray and CT images using deep learning and transfer learning algorithms,'' 2020, *arXiv:2004.00038*. [Online]. Available: http://arxiv.org/abs/2004.00038

[63] C. Zheng, X. Deng, Q. Fu, Q. Zhou, J. Feng, H. Ma, W. Liu, and X. Wang. (2020). *Deep Learning-Based Detection for COVID-19 From Chest CT Using Weak Label*. [Online]. Available: http://medRxiv:2020.03.12.20027185.

[64] O. Gozes, M. Frid-Adar, H. Greenspan, P. D. Browning, H. Zhang, W. Ji, A. Bernheim, and E. Siegel, ``Rapid AI development cycle for the coronavirus (COVID-19) pandemic: Initial results for automated detection & patient monitoring using deep learning CT image analysis,'' 2020, *arXiv:2003.05037*. [Online]. Available: http://arxiv.org/abs/2003.05037

[65] L. Li, L. Qin, Z. Xu, Y. Yin, X. Wang, B. Kong, J. Bai, Y. Lu, Z. Fang, Q. Song, K. Cao, D. Liu, G. Wang, Q. Xu, X. Fang, S. Zhang, J. Xia, and J. Xia, ``Using arti cial intelligence to detect COVID-19 and community-acquired pneumonia based on pulmonary CT: Evaluation of the diagnostic accuracy,'' *Radiology*, vol. 296, no. 2, pp. E65 E71, Aug. 2020, doi: 10.1148/radiol.2020200905.

[66] X. Yang, X. He, J. Zhao, Y. Zhang, S. Zhang, and P. Xie, ``COVID-CT-dataset: A CT scan dataset about COVID-19,'' 2020, *arXiv:2003.13865*. [Online]. Available: http://arxiv.org/abs/2003.13865

[67] X. Wang, Y. Peng, L. Lu, Z. Lu, M. Bagheri, and R. M. Summers, ``ChestX-ray8: Hospital-scale chest X-ray database and benchmarks on weakly-supervised classi cation and localization of common thorax diseases,'' in *Proc. IEEE Conf. Comput. Vis. Pattern Recognit. (CVPR)*, Honolulu, HI, USA, Jul. 2017, pp. 3462 3471, doi: 10.1109/CVPR.2017.369.

[68] (2020). *Nih Dataset*. [Online]. Available: https://www.nih.gov/news-events/news-releases/nih-clinical-center-provides-one-largest-publicly-available-chest- x-ray-datasets-scienti c-community

[69] S. Song, Y. Zheng, and Y. He, ``A review of methods for bias correction in medical images,'' *Biomed. Eng. Rev.*, vol. 1, no. 1, 2017, doi: 10.18103/bme.v3i1.1550.

[70] K. Koonsanit, S. Thongvigitmanee, N. Pongnapang, and P. Thajchayapong, ``Image enhancement on digital X-ray images using N-CLAHE,'' in *Proc. 10th Biomed. Eng. Int. Conf. (BMEiCON)*, Hokkaido, Japan, Aug. 2017, pp. 1 4, doi: 10.1109/BMEiCON.2017.8229130.

[71] K. Zuiderveld, ``Contrast limited adaptive histogram equalization,'' in *Graphics Gems IV*. New York, NY, USA: Academic, 1994.

[72] (2020). *OPENCV: Histograms-2: Histogram Equalization*. [Online]. Available: https://docs.opencv.org/master/d5/daf/tutorial-py-histogram-equalization.html

[73] O. Russakovsky, J. Deng, H. Su, J. Krause, S. Satheesh, S. Ma, Z. Huang, A. Karpathy, A. Khosla, M. Bernstein, A. C. Berg, and L. Fei-Fei, ``ImageNet large scale visual recognition challenge,'' *Int. J. Comput. Vis.*, vol. 115, no. 3, pp. 211 252, Dec. 2015, doi: 10.1007/s11263-015-0816-y.

[74] D. Su, H. Zhang, H. Chen, J. Yi, P.-Y. Chen, and Y. Gao, ``Is robustness the cost of accuracy? A comprehensive study on the robustness of 18 deep image classi cation models,'' in *Computer Vision ECCV* (Lecture Notes in Computer Science), vol. 11216, V. Ferrari, M. Hebert, C. Sminchisescu, and Y. Weiss, Eds. Cham, Switzerland: Springer, Cham, 2018, pp. 631 648, doi: 10.1007/978-3-030-01258-8_39.

[75] S. Kornblith, J. Shlens, and Q. V. Le, ``Do better ImageNet models transfer better?'' in *Proc. IEEE/CVF Conf. Comput. Vis. Pattern Recognit. (CVPR)*, Long Beach, CA, USA, Jun. 2019, pp. 2656 2666, doi: 10.1109/CVPR.2019.00277.

[76] C. Yang, Z. An, H. Zhu, X. Hu, K. Zhang, K. Xu, C. Li, and Y. Xu, ``Gated convolutional networks with hybrid connectivity for image classi cation,'' in *Proc. AAAI Conf. Arti . Intell.* New York, NY, USA: AAAI Press, 2020, pp. 12581 12588.

[77] W. Chen, D. Xie, Y. Zhang, and S. Pu, ``All you need is a few shifts: Designing ef cient convolutional neural networks for image classi cation,'' in *Proc. IEEE/CVF Conf. Comput. Vis. Pattern Recognit. (CVPR)*, Long Beach, CA, USA, Jun. 2019, pp. 7234 7243, doi: 10.1109/CVPR.2019.00741.

[78] X. Ding, Y. Guo, G. Ding, and J. Han, ``ACNet: Strengthening the kernel skeletons for powerful CNN via asymmetric convolution blocks,'' in *Proc. IEEE/CVF Int. Conf. Comput. Vis. (ICCV)*, Seoul, South Korea, Oct. 2019, pp. 1911 1920, doi: 10.1109/ICCV.2019.00200.

[79] H. Chen, Y. Wang, C. Xu, B. Shi, C. Xu, Q. Tian, and C. Xu, ``AdderNet: Do we really need multiplications in deep learning?'' in *Proc. IEEE/CVF Conf. Comput. Vis. Pattern Recognit. (CVPR)*, Seattle, WA, USA, Jun. 2020, pp. 1468 1477.

[80] Z. Chen, J. Zhang, R. Ding, and D. Marculescu, ``ViP: Virtual pooling for accelerating CNN-based image classi cation and object detection,'' in *Proc. IEEE Winter Conf. Appl. Comput. Vis. (WACV)*, Snowmass Village, CO, USA, Mar. 2020, pp. 1169 1178, doi: 10.1109/WACV45572.2020.9093418.

[81] Q. Li, L. Shen, S. Guo, and Z. Lai, ``Wavelet integrated CNNs for noise-robust image classi cation,'' in *Proc. IEEE/CVF Conf. Comput. Vis. Pattern Recognit. (CVPR)*, Seattle, WA, USA, Jun. 2020, pp. 7245 7254.

[82] P. Singh, V. K. Verma, P. Rai, and V. P. Namboodiri, ``HetConv: Heterogeneous kernel-based convolutions for deep CNNs,'' in *Proc. IEEE/CVF Conf. Comput. Vis. Pattern Recognit. (CVPR)*, Long Beach, CA, USA, Jun. 2019, pp. 4830 4839, doi: 10.1109/CVPR.2019.00497.

[83] S. Gao, M.-M. Cheng, K. Zhao, X.-Y. Zhang, M.-H. Yang, and P. H. S. Torr, ``Res2Net: A new multi-scale backbone architecture,'' *IEEE Trans. Pattern Anal. Mach. Intell.*, early access, Aug. 30, 2019, doi: 10.1109/TPAMI.2019.2938758.

[84] S. Zagoruyko and N. Komodakis, ``Wide residual networks,'' 2016, *arXiv:1605.07146*. [Online]. Available: http://arxiv.org/abs/1605.07146

[85] H. Hu, D. Dey, A. Del Giorno, M. Hebert, and J. Andrew Bagnell, ``Log-DenseNet: How to sparsify a DenseNet,'' 2017, *arXiv:1711.00002*. [Online]. Available: http://arxiv.org/abs/1711.00002

[86] L. Zhu, R. Deng, M. Maire, Z. Deng, G. Mori, and P. Tan, ``Sparsely aggregated convolutional networks,'' in *Computer Vision ECCV* (Lecture Notes in Computer Science), vol. 11216, V. Ferrari, M. Hebert, C. Sminchisescu, and Y. Weiss, Eds. Cham, Switzerland: Springer, 2018, pp. 192 208, doi: 10.1007/978-3-030-01258-8_12.

[87] X. Li, X. Song, and T. Wu, ``AOGNets: Compositional grammatical architectures for deep learning,'' in *Proc. IEEE/CVF Conf. Comput. Vis. Pattern Recognit. (CVPR)*, Long Beach, CA, USA, Jun. 2019, pp. 6213 6223, doi: 10.1109/CVPR.2019.00638.

[88] C. Liu, B. Zoph, M. Neumann, J. Shlens, W. Hua, L.-J. Li, L. Fei-Fei, A. Yuille, J. Huang, and K. Murphy, ``Progressive neural architecture search,'' in *Computer Vision ECCV* (Lecture Notes in Computer Science), V. Ferrari, M. Hebert, C. Sminchisescu, and Y. Weiss, Eds. Cham, Switzerland: Springer, 2018, pp. 19 35, doi: 10.1007/978-3-030-01246-5_2.

[89] E. Real, A. Aggarwal, Y. Huang, and Q. V. Le, ``Regularized evolution for image classi er architecture search,'' in *Proc. AAAI Conf. on Arti . Intell.*, vol. 33. Honolulu, HI, USA: AAAI Press, 2019, pp. 4780 4789, doi: 10.1609/aaai.v33i01.33014780.

[90] Y. Chen, J. Li, H. Xiao, X. Jin, S. Yan, and J. Feng, ``Dual path networks,'' in *Proc. 31st Int. Conf. Neural Inf. Process. Sys. (NIPS)*. Long Beach, CA, USA: NIPS, 2017, pp. 4470 4478.

[91] Y. Cao, J. Xu, S. Lin, F. Wei, and H. Hu, ``GCNet: Non-local networks meet squeeze-excitation networks and beyond,'' in *Proc. IEEE/CVF Int. Conf. Comput. Vis. Workshop (ICCVW)*, Seoul, South Korea, Oct. 2019, pp. 1971 1980, doi: 10.1109/ICCVW.2019.00246.

[92] J.-H. Luo, H. Zhang, H.-Y. Zhou, C.-W. Xie, J. Wu, and W. Lin, ``ThiNet: Pruning CNN lters for a thinner net,'' *IEEE Trans. Pattern Anal. Mach. Intell.*, vol. 41, no. 10, pp. 2525 2538, Oct. 2019, doi: 10.1109/TPAMI.2018.2858232.

[93] X. Li, W. Wang, X. Hu, and J. Yang, ``Selective kernel networks,'' in *Proc. IEEE/CVF Conf. Comput. Vis. Pattern Recognit. (CVPR)*, Long Beach, CA, USA, Jun. 2019, pp. 510 519, doi: 10.1109/CVPR.2019.00060.

[94] T. Shermin, S. W. Teng, M. Murshed, G. Lu, F. Sohel, and M. Paul, ``Enhanced transfer learning with imagenet trained classi cation layer,'' in *Image and Video Technology* (Lecture Notes in Computer Science), vol. 11854, C. Lee, Z. Su, and A. Sugimoto, Eds. Cham, Switzerland: Springer, 2019, pp. 142 155, doi: 10.1007/978-3-030-34879-3_12.

[95] J. Deng, W. Dong, R. Socher, L.-J. Li, K. Li, and L. Fei-Fei, ``ImageNet: A large-scale hierarchical image database,'' in *Proc. IEEE Conf. Comput. Vis. Pattern Recognit.*, Miami, FL, USA, Jun. 2009, pp. 248 255, doi: 10.1109/CVPR.2009.5206848.

[96] Petticrew, Sowden, Lister-Sharp, and Wright, ``False-negative results in screening programmes: Systematic review of impact and implications,'' *Health Technol. Assessment*, vol. 4, no. 5, pp. 1 120, 2000, doi: 10.3310/hta4050.

[97] T. Baltrusaitis, C. Ahuja, and L.-P. Morency, ``Multimodal machine learning: A survey and taxonomy,'' *IEEE Trans. Pattern Anal. Mach. Intell.*, vol. 41, no. 2, pp. 423 443, Feb. 2019, doi: 10.1109/TPAMI.2018.2798607.

[98] W. Wang, D. Tran, and M. Feiszli, ``What makes training multimodal classi cation networks hard?'' in *Proc. IEEE/CVF Conf. Comput. Vis. Pattern Recognit. (CVPR)*, Seattle, WA, USA, Jun. 2020, pp. 12695 12705.

[99] Y. Chen, C. Li, P. Ghamisi, X. Jia, and Y. Gu, ``Deep fusion of remote sensing data for accurate classi cation,'' *IEEE Geosci. Remote Sens. Lett.*, vol. 14, no. 8, pp. 1253 1257, Aug. 2017, doi: 10.1109/LGRS.2017.2704625.

[100] M. Zhang, W. Li, and Q. Du, ``Diverse region-based CNN for hyperspectral image classi cation,'' *IEEE Trans. Image Process.*, vol. 27, no. 6, pp. 2623 2634, Jun. 2018, doi: 10.1109/TIP.2018.2809606.

[101] P. Ghamisi, B. Ho e, and X. X. Zhu, ``Hyperspectral and LiDAR data fusion using extinction pro les and deep convolutional neural network,'' *IEEE J. Sel. Topics Appl. Earth Observ. Remote Sens.*, vol. 10, no. 6, pp. 3011 3024, Jun. 2017, doi: 10.1109/JSTARS.2016.2634863.

[102] J. Munro and D. Damen, ``Multi-modal domain adaptation for ne-grained action recognition,'' in *Proc. IEEE/CVF Conf. Comput. Vis. Pattern Recognit. (CVPR)*, Seattle, WA, USA, Jun. 2020, pp. 122 132.

[103] A. Khvostikov, K. Aderghal, A. Krylov, G. Catheline, and J. Benois-Pineau, ``3D inception-based CNN with sMRI and MD-DTI data fusion for Alzheimer's disease diagnostics,'' 2018, *arXiv:1809.03972*. [Online]. Available: http://arxiv.org/abs/1809.03972

[104] X. Cheng, L. Zhang, and Y. Zheng, ``Deep similarity learning for multimodal medical images,'' *Comput. Methods Biomechanics Biomed. Eng., Imag. Vis.*, vol. 6, no. 3, pp. 248 252, May 2018, doi: 10.1080/21681163.2015.1135299.

MICHAEL J. HORRY (Graduate Student Member, IEEE) received the Engineering and Laws degrees from the University of NSW, in 1998. Since that time, he has held various industry roles. He is currently an Executive Architect with IBM responsible for solution design across the partner and SI community. He is an Open Group Master Certi ed IT Architect and TOGAF 9 certi ed and a member of the Enterprise Architects Association of Australia. He has developed an interest in machine learning and particularly computer vision applications. He commenced his Ph.D. with UTS in 2020 to research automated diagnosis of pulmonary pathologies using machine learning.

SUBRATA CHAKRABORTY (Senior Member, IEEE) received the Ph.D. degree in decision support systems from Monash University, Australia. He is currently a Senior Lecturer with the School of Information, Systems, and Modeling, Faculty of Engineering and IT, University of Technology Sydney (UTS), Australia. He is also a Core Member of the Centre for Advanced Modelling and Geospatial Information Systems (CAMGIS), UTS. Previously, he worked as an academic with the University of Southern Queensland, Charles Sturt University, Queensland University of Technology, and Monash University. His current research interests include optimisation models, data analytics, machine learning, and image processing with decision support applications in diverse domains including business, agriculture, transport, health, and education. He is a Certi ed Professional Senior Member of ACS.

MANORANJAN PAUL (Senior Member, IEEE) received the Ph.D. degree from Monash University, Australia, in 2005. He was a Postdoctoral Research Fellow with the University of New South Wales, Monash University, and Nanyang Technological University. He is currently a Full Professor, the Director of Computer Vision Laboratory, and the Leader of Machine Vision and Digital Health (MaViDH) Research Group, Charles Sturt University, Australia. He has published around 200 peer reviewed publications including 72 journals. His major research interests include video coding, image processing, digital health, wine technology, machine learning, EEG signal processing, eye tracking, and computer vision. He was an invited keynote speaker in IEEE DICTA-17 & 13, CWCN-17, WoWMoM-14, and ICCIT-10. He received more than $3.6 million competitive external grant including Australian Research Council (ARC) Discovery grants, Australia-China grant. He has supervised 15 Ph.D. students to completion. He is an Associate Editor of three top ranked journals including the IEEE Transactions on Multimedia, the IEEE Transactions on Circuits and Systems for Video Technology, and the *EURASIP Journal in Advances on Signal Processing*. He was a General Chair of PSIVT-19 and a Program Chair of PSIVT-17 and DICTA-18. He was awarded the ICT Researcher of the Year 2017 by Australian Computer Society.

ANWAAR ULHAQ (Member, IEEE) received the Ph.D. degree in arti cial intelligence from Monash University, Australia. He is serving as a Lecturer with the School of Computing and Mathematics, Charles Sturt University. He has worked a Research Fellow with the Institute for Sustainable Industries and Livable Cities, Victoria University, Australia. His research interests include signal and image processing, deep learning, data analytics, and computer vision.

BISWAJEET PRADHAN (Senior Member, IEEE) received the B.Sc. degree (Hons.) from Berhampur University, India, the M.Sc. degree from IIT Bombay, Bombay, India, the M.Tech. degree in civil engineering from IIT Kanpur, Kanpur, India, and the Dresden University of Technology, Dresden, Germany, and the Ph.D. degree in GIS and geomatics engineering from the University Putra Malaysia, Serdang, Malaysia. He is currently a Distinguished Professor with the School of Information, Systems, and Modelling and the Director of Centre for Advanced Modelling and Geospatial Information Systems, University of Technology Sydney. Before joining the School of Information, Systems and Modelling, Faculty of Engineering and IT, he was a Full Professor of GIS and remote sensing with the Faculty of Engineering, Universiti Putra Malaysia. He has more than 19 years of teaching, research, and industrial experience in the eld of Geospatial Information Systems. He is listed as the World's most Highly Cited researcher by Clarivate Analytic's Report, in 2017 and 2016, as one of the world's most in uential mind. He was a recipient of Alexander von Humboldt Research Fellowship from Germany. In 2011, he received his habituation in remote sensing from the Dresden University of Technology, Germany. He was also a recipient of German Academic Exchange Research (DAAD) Fellowship Award, the Saxony State Fellowship, from 1999 to 2002, the Keith Aurtherton Research Award, and the Georg Forster Research Award from the German Government. Since February 2015, he has been serving as the Ambassador Scientist for Alexander Humboldt Foundation, Germany. He has widely travelled abroad visiting more than 55 countries to present his research ndings.

MANAS SAHA received the M.B.B.S. degree from the Dhaka Medical College, Dhaka University, in 1996, the F.C.P.S. degree in general medicine from the Bangladesh College of Physicians, the M.D. degree in nephrology from Bangabandhu Sheik Mujib Medical University, and the Ph.D. degree from Macquarie University. He is currently a Clinician Scientist, trained as a General and Renal Physician in Bangladesh and Australia. During his tenure of Ph.D., he identi ed a new underlying mechanism of hypertension and cardiovascular events in patients with CKD. He is currently working as a Staff Specialist with the Department of Medicine, Hunter New England Local Health District (HNELHD), NSW, and involving in different research groups including Machine Vision and Digital Health (MaViDH) Group, Charles Sturt University, Australia. He has been awarded Deputy Vice-Chancellor (Research) Commendation and International Society of Nephrology (ISN) Scholar. He has published many original articles in peer reviewed journals. His main research interests include cardiovascular diseases in CKD, community-based modeling for prevention of chronic disease including DM, HTN, CKD, and weight disorders, and use of arti cial intelligence in risk assessment of different diseases including cardiovascular and respiratory diseases. He is a Fellow of the Royal Australasian College of Physicians.

NAGESH SHUKLA is currently a Senior Lecturer in business analytics with the University of Technology Sydney, Ultimo, SW, Australia. He is working in the area of business data analytics, simulation modeling and optimization (applied to healthcare and supply chain/logistics management). He has contributed to more than 50 research publications in journals, conferences, patents, book chapters, and research reports. He is also a member of the editorial boards in a number of leading journals. His research interests include the development of models that deal with making complex business processes ef cient and effective, analytical models for system-level optimization and decision making, and data-driven algorithms for decision making.